Transactions of the Royal Society of Edinburgh: Earth Sciences, **81**, 251–261, 1990

An alternative astronomical calibration of the lower Pleistocene timescale based on ODP Site 677

N. J. Shackleton, A. Berger and W. R. Peltier

ABSTRACT: Ocean Drilling Program (ODP) Site 677 provided excellent material for high resolution stable isotope analysis of both benthonic and planktonic foraminifera through the entire Pleistocene and upper Pliocene. The oxygen isotope record is readily correlated with the SPECMAP stack (Imbrie *et al.* 1984) and with the record from DSDP 607 (Ruddiman *et al.* 1986) but a significantly better match with orbital models is obtained by departing from the timescale proposed by these authors below Stage 16 (620 000 years). It is the stronger contribution from the precession signal in the record from ODP Site 677 that provides the basis for the revised timescale. Our proposed modification to the timescale would imply that the currently adopted radiometric dates for the Matuyama–Brunhes boundary, the Jaramillo and Olduvai Subchrons and the Gauss–Matuyama boundary underestimate their true astronomical ages by between 5 and 7%.

KEY WORDS: Pleistocene timescale, Milankovitch, astronomical chronology, oxygen isotopes, SPECMAP, magnetostratigraphy.

It has long been recognised that in most areas of the ocean the accumulation rate of the sediment is too low to permit the recovery of an accurate first-order record of Pleistocene climatic variability (Emiliani 1955; Shackleton & Opdyke 1973; Peng *et al.* 1977; Morley & Shackleton 1984). A useful criterion for establishing the potential of the sedimentary record of an area is that the five discrete substages of Stage 5 (Shackleton 1969), which are generally accepted as having resulted from the precession cycle during an interval of high orbital eccentricity (Broecker *et al.* 1968), should be well represented. In the Atlantic, several areas satisfy this criterion (e.g. the equatorial Atlantic – Emiliani 1955; the North Atlantic – Emiliani 1958; the East Atlantic – Shackleton 1977; the South East Atlantic – Morley & Shackleton 1984). In the other oceans the Subantarctic has provided good records (Hays *et al.* 1976; Nelson *et al.* 1986). In the low-latitude Pacific the only excellent records come from the eastern side (Ninkovitch & Shackleton 1975; Shackleton & Pisias 1985). Examination of the record at Deep Sea Drilling Project (DSDP) Site 504 showed that long, detailed records could be obtainable in that area but unfortunately the recovery at that site was not adequate for continuous detailed analysis (Shackleton & Hall 1983). ODP Site 677 was cored using the Advance Piston Corer (APC) at 1°12′N, 83°44′W in 3461 m water depth (Becker *et al.* 1988), a location very close to DSDP Site 504. Two holes, 677A and 677B, were recovered with the objective of obtaining a complete Plio–Pleistocene record (Shipboard Scientific Party, 1988).

A very unusual advantage of the sediments at this site is that it has proved possible to generate virtually complete oxygen isotope records for both *Globigerinoides ruber*, a surface-dwelling planktonic species, and benthonic species (in most samples, *Uvigerina senticosa*). Analytical data are available in Shackleton and Hall (1989); additional measurements are given in Appendix 1. These additional measurements are of samples for Hole 677B that were obtained in order to cover the inter-core gaps in Hole 677A.

1. Physical stratigraphy

Figure 1 shows the oxygen isotope record versus adjusted depth for Holes 677A and 677B. Depth adjustments to each successively deeper APC core must be made because the nominal depth relationships (deriving from the progressive lowering of the drill string in 9·5 metre steps, and the addition of sections of pipe to increase its length) are subject to various uncertainties that arise because the drill string is not perfectly rigid, nor is the drill ship perfectly stationary. Ruddiman *et al.* (1987) have given an excellent summary of the difficulties that ensue. Like Alexandrovich and Hays (1989), we used data from DSDP504 (Shackleton & Hall, 1983) as well as our data from ODP677B to construct the best set of depth adjustments to the primary ODP677A data set (Table 1). The figures in Table 1 differ from those in Shackleton and Hall (1989) as follows. At about 17 m between 677A cores 2 and 3 (Stage 12), a small gap is inserted on the basis of the thickness of stage 12 at DSDP504. At about 27 m between 677A cores 3 and 4, we have slightly extended the 677B data; agreement with 504 is excellent but it is now certain that the upper part of 677A core 4 is disturbed. We now have overlapping data from hole 677B covering the gaps between hole 677A cores 4 and 5; 5 and 6; 6 and 7; and 7 and 8 (Appendix 1). The overlaps were checked by aligning core photographs (Shipboard Scientific Party, 1988). Our adjustments are not identical with those proposed by Alexandrovich and Hays (1989) probably largely because our data are spaced at 10 cm whereas their data were mainly collected at 50 cm intervals, and this has provided a substantially firmer basis for correlating the holes in detail.

2. Correlation to other records

Oxygen isotope stages as defined by Emiliani (1955), Shackleton and Opdyke (1973) and Ruddiman *et al.* (1986) are readily recognized and for orientation are indicated on

Table 1 Depth adjustments used to construct a continuous record by combining data from ODP677A and ODP677B

Sample	ODP depth (m)	Adjusted depth (m)
111-677A-1-1, 40-42	0·40	0·40
111-677A-1-5, 10-12	6·10	6·10
111-677A-2-1, 29-41	6·59	7·84
111-677A-2-7, 58-60	15·78	17·03
111-677A-3-1, 10-12	15·80	17·35
111-677A-3-7, 59-61	25·29	26·84
111-677A-4-1, 8-10	25·28	28·03
111-677A-4-6, 140-142	34·10	36·85
111-677A-5-1, 10-12	34·80	35·95
111-677A-5-7, 30-32	44·00	45·15
111-677A-6-1, 10-12	44·30	46·15
111-677A-6-7, 60-62	53·79	55·64
111-677A-7-1, 10-12	53·80	56·60
111-677A-7-7, 48-50	63·18	65·98
111-677A-8-1, 10-12	63·30	67·30
111-677A-8-7, 30-32	72·50	76·50
111-677A-9-1, 0-2	72·70	76·70
111-677A-9-6, 140-142	81·60	85·60
111-677A-10-1, 0-2	82·20	86·20
111-677A-10-7, 50-52	91·70	95·70
111-677A-11-1, 0-2	91·72	95·72
111-677A-11-7, 60-62	101·30	105·30
111-677A-12-1, 0-2	101·20	107·20
111-677A-12-7, 60-62	110·80	116·80
111-677A-13-1, 1-3	110·71	116·71
111-677A-13-7, 50-52	120·20	126·20
111-677B-1-1, 0-2	0·01	0·81
111-677B-1-6, 10-12	7·61	8·41
111-677B-2-1, 10-12	7·71	7·71
111-677B-2-7, 10-12	16·71	16·71
111-677B-3-1, 10-12	17·21	19·21
111-677B-3-7, 60-62	26·71	28·71
111-677B-4-1, 20-22	26·81	30·36
111-677B-4-cc-30-32	36·31	39·86
111-677B-5-1, 30-32	36·41	39·96
111-677B-5-7, 50-52	45·61	49·16
111-677B-6-1, 10-12	45·71	50·15
111-677B-6-cc-30-32	55·36	59·81
111-677B-7-1, 30-32	55·41	58·91
111-677B-7-cc-25-27	65·16	68·66
111-677B-8-1, 60-62	65·21	70·51
111-677B-8-6, 90-92	73·01	78·31
111-677B-9-1, 10-12	74·21	77·21
111-677B-9-cc-30-32	83·41	86·41

Figure 2 where the records of Holes 677A and 677B are combined. Of particular importance is the documentation of that part of the record deposited during the Jaramillo subchron. Figure 3 shows the oxygen isotope data for equivalent parts of DSDP Site 552A (Shackleton *et al.* 1984), DSDP607 (Ruddiman *et al.* 1986) and ODP677 together with the magnetic stratigraphy (limits of the Jaramillo Subchron) for DSDP552A and DSDP607. The isotope stages numbered down to Stage 33 by Ruddiman *et al.* (1986) are clearly recognisable in all three records.

In the lower part of the Pleistocene we have five biostratigraphic datums that have been accurately determined in this site (Table 2). These serve to validate the stage numbers assigned (which we regard as being defined in DSDP607 by Ruddiman *et al.* (1986) for this interval). In particular since the same datums have all been determined in core V28-239, for which good magnetostratigraphy is available (Shackleton & Opdyke 1976), they provide support for our stage numbering to the critical Stage 63, which has at its base the reversal marking the top of the Olduvai chron (Ruddiman *et al.* 1986). Figure 4 shows the position of each biostratigraphic datum (from Table 2), the stage numbers for the lower part by correlation with the record of DSDP Site 607 (Ruddiman *et al.* 1986) and the implied stratigraphic positions of the relevant magnetic reversals.

In the upper Pliocene section we rely heavily on DSDP Site 607. Raymo *et al.* (1990) have already shown correlations between the two sites over this interval and since Hole 677B does not provide overlapping data below 70 m there is no basis for major modification of the proposed relationships. The data are shown in Figure 2 to 120 m although we only discuss them to Stage 104 in which the Gauss–Matuyama boundary is located at DSDP Site 607.

3. Astronomical chronology

The hypothesis that variations in the earth's orbital geometry are responsible for the timing of climatic change has been under consideration for almost two centuries and was formulated in a modern manner early in this century (Milankovitch 1930). However, it was Hays *et al.* (1976) who provided the first clear documentation that the geological record does reveal the independent contributions of the three orbital elements to the determination of past climate. Imbrie *et al.* (1984) generated a stacked $\delta^{18}O$ record for the past 800 ka (thousand years) and used astronomical data to fine-tune the geological timescale, and Martinson *et al.*

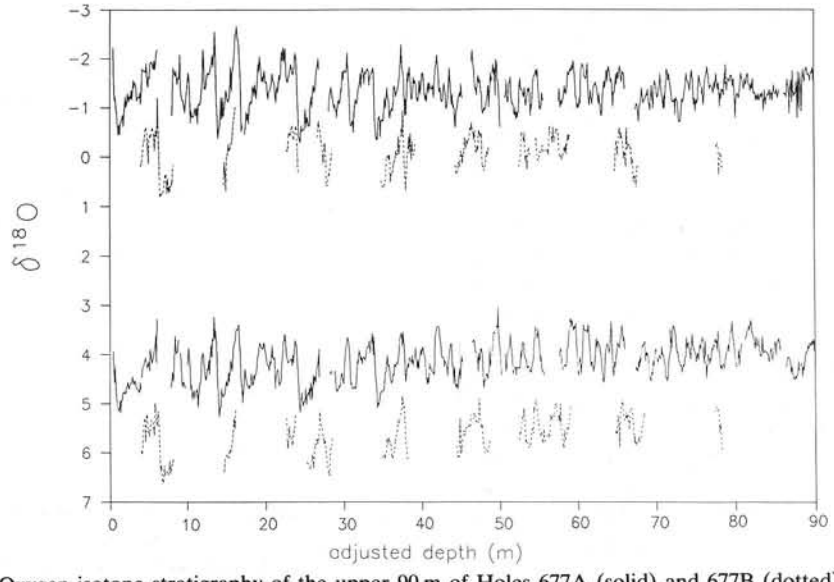

Figure 1 Oxygen isotope stratigraphy of the upper 90 m of Holes 677A (solid) and 677B (dotted): above, planktonic; below, benthonic. The data for Hole 677B have been offset by 1·5 per mil for clarity.

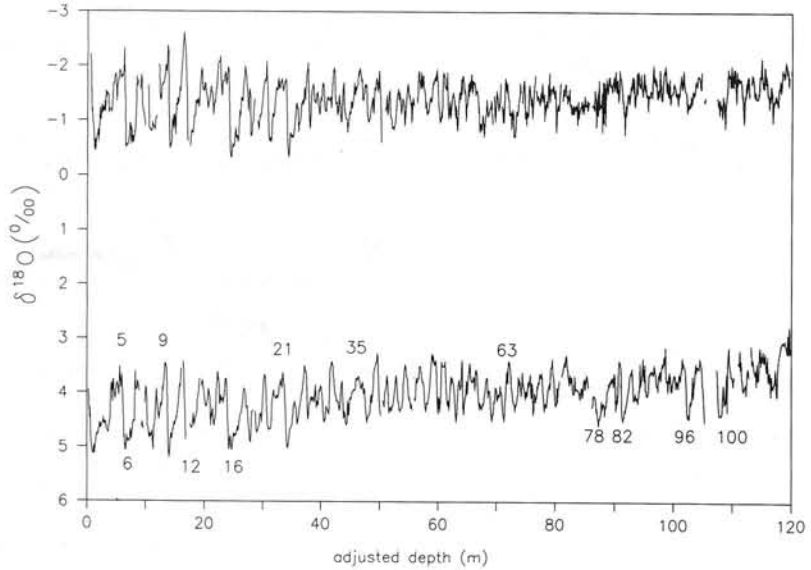

Figure 2 Oxygen isotope stratigraphy combining Holes 677A and B: above, planktonic; below, benthonic, to 120 m. Selected isotope stages are labelled for orientation.

(1987) discussed several strategies for accomplishing this objective. We consider that the time-calibration obtained by Martinson *et al*. (1987) for the past 300 ka, based on several excellent data sets, is correct within the rather narrow limits that they specify. A convincing test and validation of the stacking approach is to regard the stacked record as a prediction that can be tested by obtaining a very detailed record and comparing it with the stack of less detailed records; the high resolution record of core V19-30 shown by Shackleton and Pisias (1985) provides a test of the validity of the stack produced by Pisias *et al*. (1984) and used by Martinson *et al*. (1987). Back to about 620 ka the data sets used by Imbrie *et al*. (1984) are of good quality and are corroborated by more recent data (Prell *et al*. 1986) and the data presented here. It is remarkable, for example, how similar the data presented here are to the stacked record for stages 13–15. However below this point there are serious discrepancies between the data sets used by Imbrie *et al*. (1984) and by Prell *et al*. (1986), which lead to difficulties in developing a tuned timescale. Ruddiman *et al*. (1986) have made an attempt to improve the astronomical calibrations proposed by Imbrie *et al*. (1984) in the interval of time between 620 ka and 800 ka. In this paper we re-examine astronomical calibrations over this interesting interval, during which the climate system underwent a major change from a regime in which the response was dominated by a 41 ka periodicity attributed to obliquity forcing (Ruddiman *et al*. 1986), to a regime characterised by 100 ka cycles that are loosely associated with the eccentricity cycle (Imbrie *et al*. 1984).

The basic features of the variations in earth orbital geometry that affect the seasonal and latitudinal distribution of solar energy at the earth's surface are now well known (Berger 1976, 1988). It is widely believed that future improvements in astronomical theory or computational methods will not significantly change the data already available for the past million years or so (Berger 1984; Berger & Loutre 1988; Berger 1989). For the more remote geological past, the actual insolation values as a function of time eventually become indeterminate although the basic periodicities are stable. We used the algorithm of Berger (1978) in the early stages of this work. The results shown here are based on newer calculations (Berger & Loutre 1988; Berger 1989), but it should be emphasised that the substantial changes in timescale that we propose are not caused by our using these calculations. The new calculations diverge from the old ones to an extent that would affect correlations with the geological record to a significant extent at about 1·5 Ma (Million years) (Berger 1989), although by around 2·0 Ma the results differ in a major way. On the other hand the major revision that we propose here depends

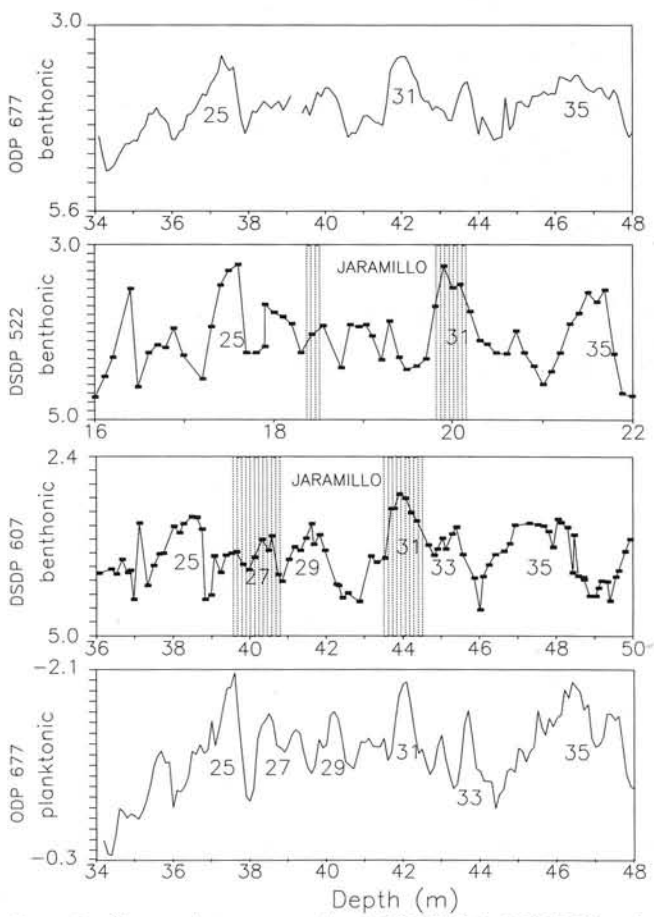

Figure 3 Oxygen isotope records of DSDP552A, DSDP607 and ODP677 for the interval of Stages 24 to 32. Shaded intervals indicate the uncertainty limits of the boundaries of the Jaramillo in DSDP552A (Shackleton *et al*. 1984) and DSDP607 (Ruddiman *et al*. 1986).

Table 2 Biostratigraphic Datums at Site 677

Datum (LAD = Last Appearance Datum)	Adjusted depth (m)
Helicosphaera sellii LAD[1]	62·6
Calcidiscus macintyrei LAD[1]	65·3
Gephyrocapsa oceanica LAD[2]	68·2
Pterocanium prismatium LAD[3]	70·6
Globigerinoides fistulosus LAD[4]	70·6

[1] J. Backman personal communication (1988).
[2] I. Raffi personal communication (1989).
[3] J. Alexandrovich (1989).
[4] Shackleton & Hall (1989).

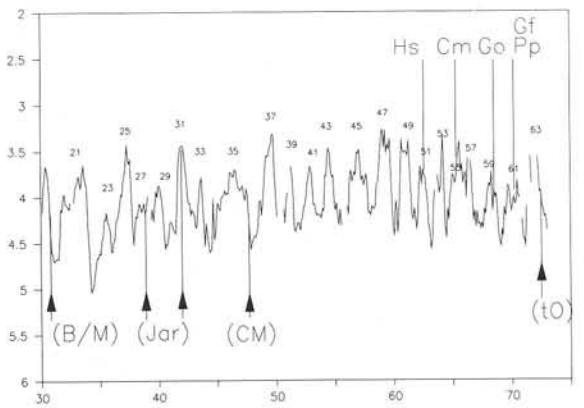

Figure 4 Benthonic oxygen isotope record of Site 677 from 30 to 75 m. Hs: upper limit of *Helicosphaera sellii*; Cm: upper limit of *Calcidiscus macintyrei*; Go: upper limit of *Gephyracapsa oceanica*; Gf: upper limit of *Globigerinoides fistulosus*; Pp: upper limit of *Pterocanium prismatium*. Upward pointing arrows show the approximate stratigraphic levels corresponding to magneto-stratigraphic events; (B/M): base of Brunhes normal chron; (Jar): boundaries of the Jaramillo normal subchron; (CM): Cobb Mountain normal event; (tO): upper boundary of Olduvai normal subchron.

on a new interpretation of the records over the interval between about 0·6 and 1·2 Ma where one would obtain almost identical age estimates whether one used the calculations of Berger (1978) or the newer ones of Berger and Loutre (1988).

4. Methods

Oxygen isotope data for Hole 677A and Hole 677B were combined after making the depth adjustments discussed above. Unfortunately an unexplained analytical offset occurred in the analysis of samples from Hole 677B which were made immediately after delivery of a new mass spectrometer. To take account of this, 0·2 per mil was added to $\delta^{18}O$ values for benthonic species in Hole 677B cores 2 to 7. The section of 677A covering Stage 5 was eliminated beause the record from 677B is clearly superior and this part of Hole 677A is probably significantly disturbed. A conventional piston core would probably provide a far better record of the upper 10–20 m of the section, and we have devoted minimal effort to this part of the section. Data from the top metre of 677A core 4 were discarded due to obvious disturbance and physical mixing. The sections of 677B below 70 m were not used but virtually all the remaining overlapping data could be combined satisfactorily. Duplicate measurements at the same depth were averaged, except that if a replicate analysis was made because the result of the initial measurement was suspect, and if the second measurement confirmed that the first one was incorrect, the second alone was used (fewer than 1% of the measurements made have been discarded).

As each version of the age model was developed, the age of every sample was estimated by linear interpolation between the control depths (see below). Values were then estimated at uniform 3 ka intervals using a Gaussian weighting method that introduces a small amount of smoothing. This interpolated data set was used for statistical analysis. Spectra and coherencies were calculated using standard methods (Jenkins & Watts 1968; Imbrie *et al.* 1984). All the estimates shown here were made with 80 lags after the data had been linearly detrended.

The records that were carefully documented by Ruddiman *et al.* (1986) are very clearly dominated by cycles with a period near 41 ka. The record from Site 677 is similarly dominated by cycles with a wavelength (in depth terms) of around 1·6 to 1·8 m over the interval from about 45 m to 65 m. The transitional interval at Site 677 is especially interesting because it displays a clearly visible secondary cycle with a shorter wavelength of a little under 1 m, which is probably associated with forcing by precession. Because the effect of precession on the seasonal distribution of solar insolation is modulated by the eccentricity cycle, the precession component of the record provides a better tool for accurate correlation than the more regular obliquity cycle.

Spectral analysis of the $\delta^{18}O$ data as a function of depth confirms the visual evidence for this cyclicity. In Figure 5 we show the result of filtering the data set in the depth domain using bandpass filters designed to capture each of the two cycles. If it is assumed that the 1·6 m cycle (which is clearly recognisable in dark–white alternations on the core photographs) is derived from the 41 ka obliquity cycle, it is apparent that the modulation on the shorter 1·0 m cycle is consistent with a derivation from the eccentricity cycle that provides the envelope for the climatic precession signal. It is a relatively straightforward process to iteratively generate a timescale for the record that brings the observed cycles into phase with the inferred astronomical forcing. In this paper we proceed on the simplest assumption, that the climate system as it is monitored by the ocean $\delta^{18}O$ record, has responded to forcing by insolation variations with the same time-constant throughout the interval under discussion. We have experimented with several procedures for generating the timescale starting with this assumption. In this paper we proceed by using the simple model described by Imbrie and Imbrie (1980) as a tuning target. However, it is important to examine those sections of the record that have been of special significance in leading to our conclusion, in the first

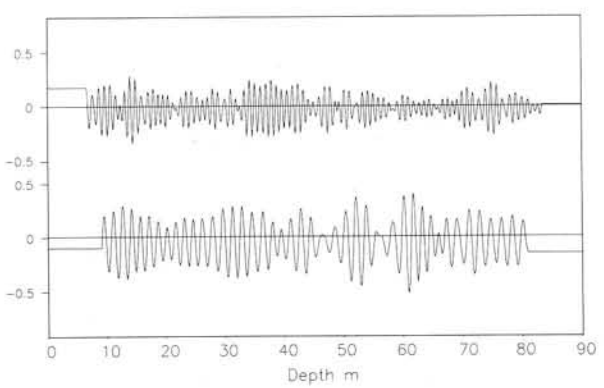

Figure 5 Oxygen isotope record for Site 677 (Fig. 2) filtered in the depth domain with filters having central frequencies of 1 cycle per 0·9 m for the planktonic record (above) and 1 cycle per 1·6 m for the benthonic record (below).

instance by looking at the result of filtering in the depth domain (Figure 5). An analogous procedure was used by Ruddiman *et al.* (1986).

The output resulting from filtering the data in the depth domain with a filter designed to capture the 1·6 m cycle is remarkably regular to about 78 m, aside from three intervals: around 40 m, 47 m and 65 m. At 40 m the output from the 'precession' filter is rather regular, suggesting that there is no major distortion of the sedimentary record. At 47 m (Stage 35) the uncertainty is more acute. The thickness of Stage 35 is clearly more comparable to the thickness of two average cycles above or below this point than to one. In DSDP607 stage 35 is also anomalously thick for a single 41 ka cycle; on the other hand in DSDP552A its presumed correlative is rather similar to adjacent cycles. In favour of assigning to Stage 35 the two 41 ka cycles implied by its thickness, is the fact that the planktonic signal in the lower part of the stage contains distinct 1-m scale structure that would not be of appropriate timescale if the whole were compressed into a single 41 ka cycle. At 65 m the irregularity derives from the poor development of Stage 56.

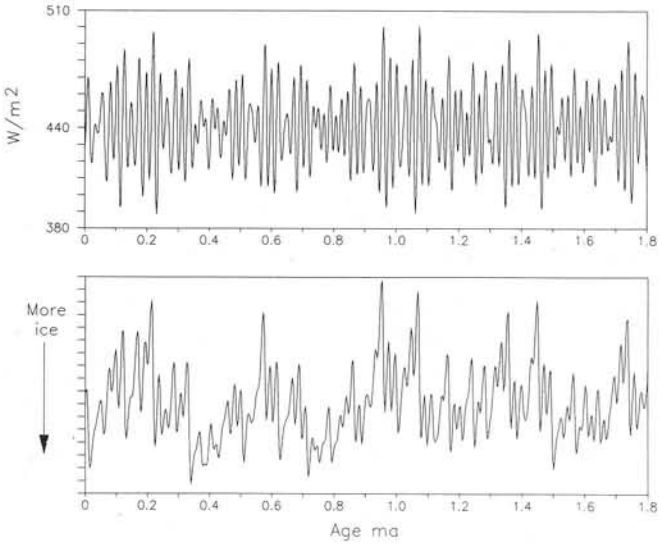

Figure 6 Insolation at 65°N in July for the past 1·8 Ma (above, from Berger & Loutre, 1988) and ice volume model (arbitrary scale) run using the model of Imbrie and Imbrie (1981) (below).

This stage is also poorly developed in DSDP607 (that is, the $\delta^{18}O$ value is not so positive as in other glacial stages and the interval with glacial $\delta^{18}O$ values is relatively thin), but the records of 677 and 607 are remarkably similar and there seems little doubt that the representation is correct; the thickness in 607 and in core V28-239 supports the conclusion drawn by Ruddiman *et al.* (1986), that two tilt cycles are represented. The core photographs of both 677A and 677B show distinct dark–light cycles in this part of the record with a wavelength somewhat less than 1 m. If these represent precession cyles, they suggest that the accumulation rate was just a little below average here.

Figure 6 shows the July 65°N insolation record for the past 1·6 Ma, together with an ice volume simulation using the model of Imbrie and Imbrie (1980). At the outset we chose to use the latter as our tuning target because it has proved a convenient target in the upper part of the record (Martinson *et al.* 1987). The model has two variable parameters: the time-constant for ice-sheet response, and the ratio of growth response-time (dependent on snow accumulation) to decay response-time (dependent on ice melting). We anticipated that the older part of the record in Site 677 might require a change in one of these parameters, but in fact the data for the lower part of the record that we have examined fit the model even better than the data for the time interval for which the parameters were originally specified by Imbrie and Imbrie (1980). For this reason we have continued to work with the model using the same parameters throughout this study despite the logical inconsistency in assuming identical model parameters for a long interval during which the characteristic scale of ice sheets must have increased significantly.

Figure 7 shows the planktonic and benthonic data on a timescale derived by matching to this record in a manner consistent with the implications of the filtering experiment. Procedurally this timescale was developed so as to align features in the planktonic $\delta^{18}O$ record with features in the target, by iteratively assigning age control points and by assuming uniform accumulation between these points. Table 3 lists the control points used.

Over the time interval 640 ka to 1·6 Ma cross-spectral analysis (Fig. 8, above left) shows that our planktonic data has proportionally slightly less power at precessional frequencies relative to tilt than the model. However, overall

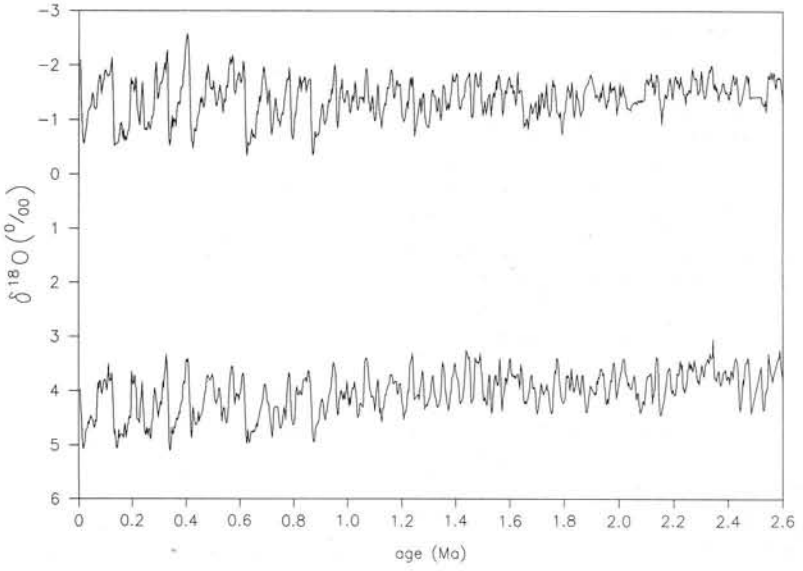

Figure 7 Planktonic and benthonic oxygen isotope data for ODP677 for the past 2·6 Ma after tuning the planktonic record to the target illustrated in Figure 6.

the spectral distribution in the data for this time interval is closer to that of the model than it is for the last 600 ka, for which the model was developed. This is because the enormous concentration of power at the 100 ka wavelength which dominates the record of the last 600 ka, and which is not adequately predicted by the model of Imbrie and Imbrie (1980), is absent in the record from 640 ka to 1·6 Ma. Coherency between model and data is 0·95 in the obliquity band and 0·94 and 0·96 for the precession peaks. The benthonic data displays even higher coherency (0·97) with the model over the obliquity band (Fig. 8, above right) and although this data set contains a smaller precession component it is also significantly coherent (0·91 and 0·77) with the main components of climatic precession. We do not show phase spectra since our tuning procedure is designed to achieve a zero phase relationship.

In the interval between 1·6 Ma and 2·6 Ma we interpret the sequence of obliquity cycles in the same way as Raymo *et al.* (1989) and Raymo *et al.* (1990). We have not taken orbital tuning to such detail in this part of the record, largely because of deficiencies in the planktonic $\delta^{18}O$ record. There are intermittent intervals over which the planktonic record departs markedly from the benthonic one and in some intervals the planktonic data are very noisy. It is possible that this arises as a result of slight diagenetic alteration in the thinner-walled planktonic specimens. Despite the reduced quality of the data, coherency with the precessional component of the tuning target is highly significant: 0·87 and 0·91 for the planktonic (Fig. 8, below left), 0·88 and 0·92 for the benthonic (Fig. 8, below right). Over this interval the benthonic data are again more highly coherent with the orbital data in the obliquity band (0·94) than are the planktonic data (0·89).

In Figure 9 the planktonic data are filtered in the time

Table 3 Age control points inserted to develop the age model

Depth (m)	Age (Ma)	Depth (m)	Age (Ma)
0·00	0·00	50·10	1·248
0·40	0·006	51·40	1·280
3·80	0·061	52·90	1·315
4·90	0·085	53·59	1·335
6·10	0·122	54·59	1·355
8·17	0·194	56·79	1·398
9·05	0·214	59·50	1·449
10·20	0·238	60·70	1·471
12·02	0·286	61·29	1·490
12·30	0·295	61·50	1·499
13·54	0·329	63·05	1·532
14·04	0·339	63·99	1·564
16·34	0·405	64·50	1·572
17·40	0·428	65·29	1·603
18·65	0·459	66·49	1·641
19·25	0·481	67·09	1·650
19·85	0·501	67·80	1·668
20·25	0·509	69·90	1·716
21·25	0·534	70·69	1·736
22·50	0·573	71·40	1·757
22·70	0·582	72·89	1·788
23·25	0·595	73·89	1·809
23·50	0·602	74·60	1·829
23·85	0·616	75·89	1·851
24·40	0·626	76·29	1·880
26·74	0·688	76·69	1·910
27·50	0·709	77·69	1·944
30·43	0·784	79·55	1·983
32·40	0·821	81·99	2·021
33·75	0·860	87·39	2·079
37·49	0·953	89·99	2·155
38·39	0·976	90·69	2·131
39·09	0·996	91·69	2·147
39·49	1·005	93·00	2·187
40·09	1·027	95·19	2·231
40·59	1·033	97·69	2·304
41·99	1·069	98·69	2·346
42·89	1·089	100·29	2·388
43·55	1·111	101·49	2·428
44·33	1·125	104·99	2·479
45·41	1·145	107·55	2·523
46·45	1·163	109·59	2·550
47·03	1·172	111·55	2·594
47·89	1·209	113·29	2·635
49·60	1·240	142·80	3·160

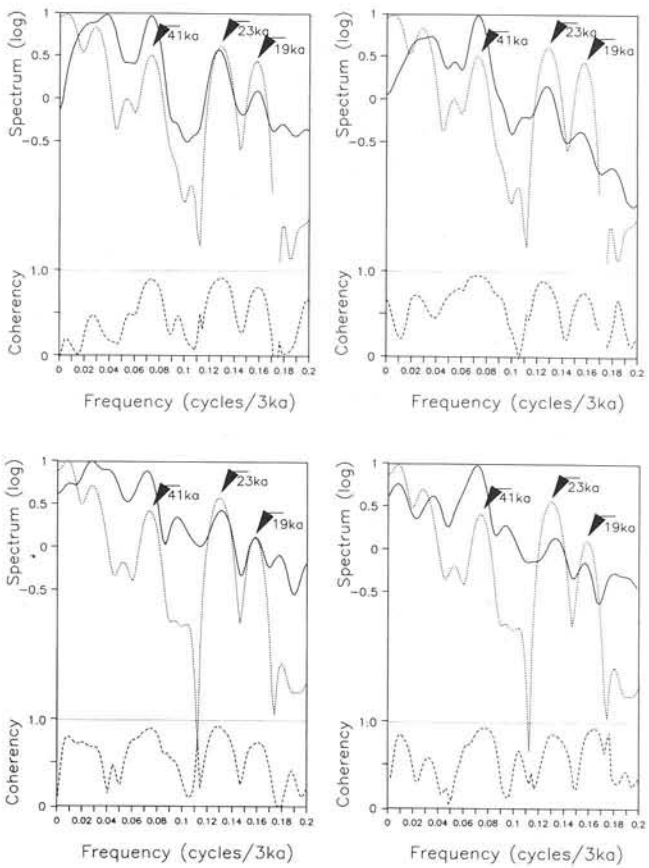

Figure 8 Cross-spectral comparison of (dotted) the model (from Fig. 6, below) and (solid) the data (from Fig. 7). Above left: planktonic, 639 ka to 1·599 Ma; above right: benthonic 639 ka to 1·599 Ma; below left: planktonic, 1·599 to 2·598 Ma; below right: benthonic, 1·599 to 2·598 Ma. Coherency is shown (dashed) in the lower part of each panel and is high at the obliquity and precession frequencies in all four plots.

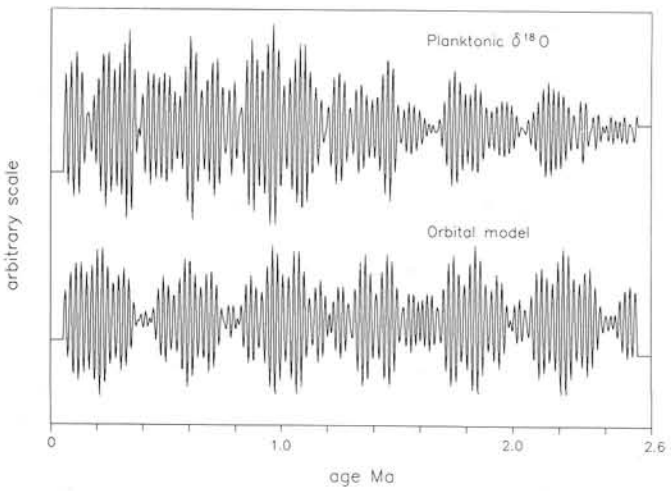

Figure 9 Oxygen isotope record for planktonic foraminifera in Site 677 (Fig. 7) filtered in the time domain and compared with the model (Fig. 6, below) similarly filtered. The filter used has a central frequency of 0·045 c/ka and a bandwidth of 0·036 c/ka.

domain for comparisons with filtered components of the modelled record. The resemblance between the eccentricity modulation of the precessional component in the model output, and the modulation on the filtered planktonic data, is remarkable and it seems very unlikely that this match could have been obtained with an incorrect timescale.

5. Discussion

The chronology that we have developed may be used to estimate the ages of the last six major reversals of the Earth's magnetic field. Table 4 compares our ages with currently accepted geochronological estimates, and with the figures given by Ruddiman *et al.* (1989) and Raymo *et al.* (1989). Our estimates differ from those of Ruddiman *et al.* (1986, 1989) as a result of three divergences between our interpretation and theirs. First, we have inferred an extra tilt cycle in the lower Brunhes. For this interval our solution resembles that proposed by Johnson (1982). Second, we have interpreted Stage 21 as containing three precession peaks where Ruddiman *et al.* (1986) compressed this stage into a single tilt cycle. Third, we have interpreted Stage 35 as representing more than a single tilt cycle. The first of these conclusions would perhaps have been drawn by Ruddiman *et al.* (1986) had they proceeded, as we did, by initially filtering entirely in the depth domain. However they chose to filter after setting literature ages for the magnetic reversals, so that their procedure is only analogous to ours for the interval of Stages 32 to 64. As discussed above, their data is open to the interpretation that we propose for this section (that is, their Stage 35 is significantly thicker than would be predicted by their interpretation). As mentioned above, our interpretation of the interval between Stages 71 and 104 is consistent with that of Raymo *et al.* (1989) and Raymo *et al.* (1990). Thus in Table 4 our estimate for the interval of time between the top of the Gauss chron and the base of the Olduvai subchron is essentially the same as estimated by Raymo *et al.* (1989).

A revision of the ages of the most recent three reversals could possibly be accommodated by an assumption that the

Table 4 Comparison of our estimates and those previously obtained for selected magnetic reversal boundaries

Isotope stage	Correlative reversal	Age[1]	Age[2]	Age[3]
base 19	base Brunhes	0·73	0·73	0·78
mid 27	top Jaramillo	0·92	0·90	0·99
mid 31	base Jaramillo	0·98	0·97	1·07
base 35	Cobb Mountain	1·10	1·10	1·19
base 63	top Olduvai	1·66	1·65	1·77
base 71	base Olduvai[4]	1·88	1·82	1·95
104	top Gauss	2·47	2·48	2·60

[1] From Berggren *et al.* (1985) and Maniken & Grommé (1982).
[2] Ruddiman *et al.* (1989); Raymo *et al.* (1989).
[3] This work.
[4] Since Ruddiman *et al.* (1986) discuss two alternative positions for the base of the Olduvai it should be mentioned that in most deep-sea cores the extinction of *Discoaster brouweri* is very close to the base of the Olduvai (Backman & Shackleton 1983) and that this event is identified with the base of Stage 71 both in DSDP607 as Ruddiman *et al.* (1986) finally determined it, and in ODP677 (A. Chepstow-Lusty, pers. comm. 1989).

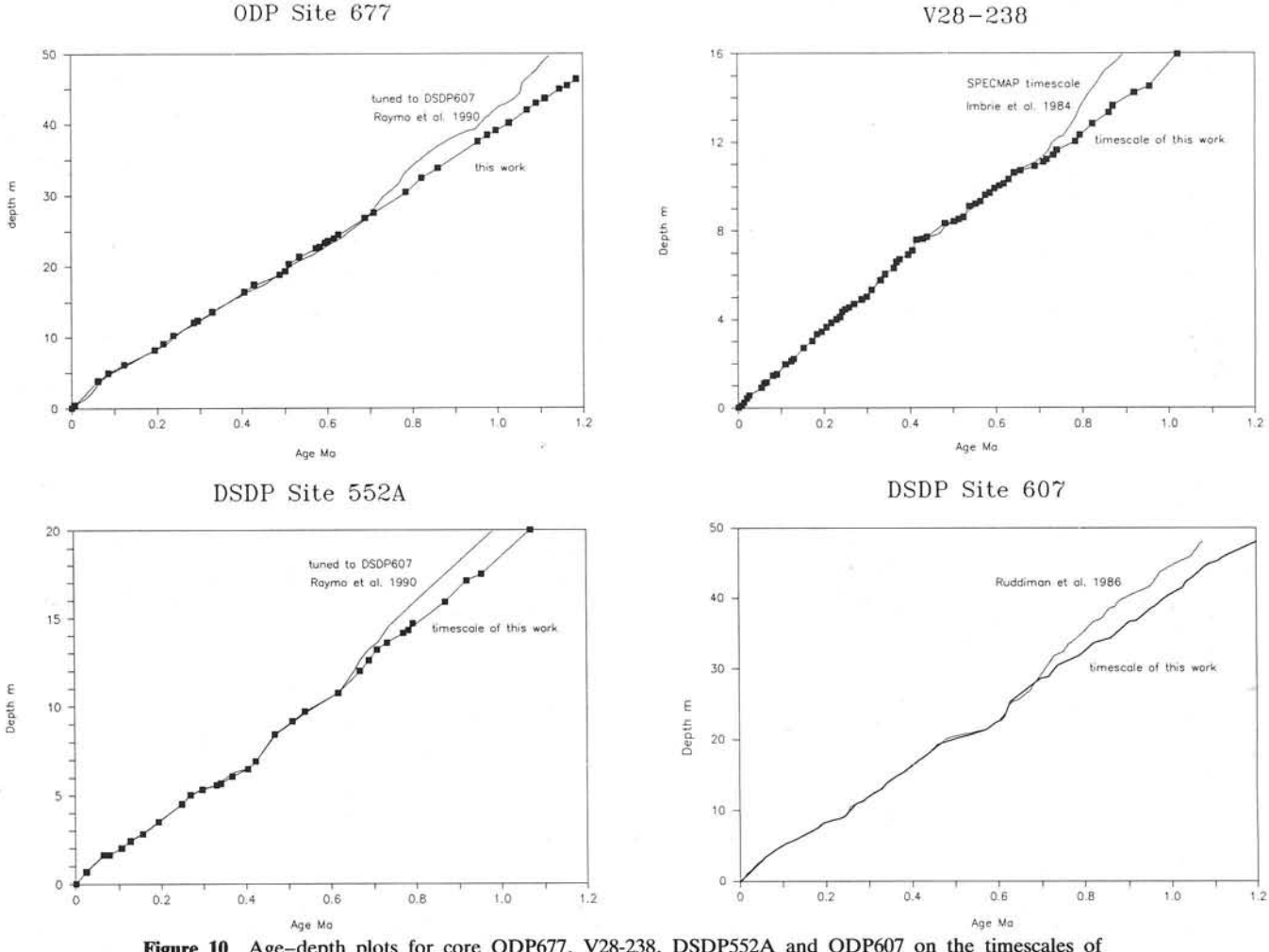

Figure 10 Age–depth plots for core ODP677, V28-238, DSDP552A and ODP607 on the timescales of Raymo *et al.* (1990), SPECMAP (Imbrie *et al.* 1984), and Ruddiman *et al.* (1986), compared with age-depth plots using the timescale of this work.

relatively limited number of measurements are systematically in error at the young end of the K/Ar timescale. However, if the older reversals are also older than currently believed it is perhaps more likely that the decay constant generally adopted (Steiger & Jäger 1977) is in error. This conclusion would be consistent with that reached by Hilgen and Langereis (1989), who argue that the duration of the interval from the top of the Gilbert Chron to the base of subchron C1 is greater than currently believed.

Support for our interpretation of the critical interval between Stages 15 and 22 comes from examination of accumulation rates. Figure 10 compares accumulation rates of four cores on conventional timescales and on the one proposed here. Core V28-238 was used as the reference core in the studies of Imbrie *et al.* (1984) and of Prell *et al.* (1986) because it was regarded as the core with the most uniform accumulation rate of all those for which data were available. DSDP Site 552A is from Rockall at 55°N in the North Atlantic (Shackleton *et al.* 1984) and DSDP607 from the mid-Atlantic Ridge at 40°N (Ruddiman *et al.* 1986). In each case, the previous timescale requires greater changes in accumulation rate than are implied by our new timescale. Although a systematic change in accumulation rates at the inception of larger scale glaciation might be expected, a change in accumulation rate in the same direction over a limited time interval in four such different depositional settings in two ocean basins does seem unlikely.

6. Conclusions

Both the effect of changes in the obliquity of the ecliptic, and of axial precession together with its modulation by eccentricity variations, are clearly present in the Quaternary and late Pliocene oxygen isotope records from ODP Site 677. A timescale has been developed on the assumption that there has been a consistent phase relationship between the astronomical forcing and the climatic response over the past 2·6 Ma. This timescale demonstrates coherencies between modelled and observed variations for the whole of the past 1·6 Ma that are as high as those previously observed for the last 0·6 Ma, while for the previous million years (2·6–1·6 Ma) they are almost as high. However, the timescale developed requires ages for the last few reversals of the Earth's magnetic field that are around 5–7% greater than the currently accepted values.

7. Acknowledgements

This work was supported by NERC grants GR3/3606 and GST/02/260 to N.J.S. and CEA grant BC-4561 to A.B. We are grateful to M. A. Hall, A. Chepstow-Lusty, J. Proud and S. Crowhurst for assistance in Cambridge, and to M. F. Loutre for assistance in Louvain La Neuve. We are grateful to N. Pisias for assistance in setting up the programs for spectral analysis in Cambridge, and for his encouragement. Reviews from J. Imbrie and M. Raymo and intensive discussions with J. Alexandrovich, F. J. Hilgen, J. Imbrie, G. J. Kukla, D. G. Martinson, D. P. McKenzie, and G. Weedon enabled us to significantly improve the original manuscript.

8. References

Alexandrovich, J. 1989. Radiolarian Biostratigraphy of Site 677, Eastern Equatorial Pacific. Late Miocene through Pleistocene. PROC ODP, SCI RESULTS **111,** 245–62.

Alexandrovich, J. & Hays, J. D. 1989. High-resolution stratigraphic correlation of ODP Leg 111 Holes 677A and 677B and DSDP Leg 69 Hole 504. PROC ODP SCI RESULTS **111,** 263–85.

Backman, J. & Shackleton, N. J. 1983. Quantitative biochronology of Pliocene and early Pleistocene nannofossils from the Atlantic, Indian and Pacific oceans. MAR MICROPALEONTOL **8,** 141–70.

Becker, K., Sakai, H. *et al.* 1988. PROC ODP INIT REPTS (Pt A), **111**

Berger, A. 1976. Obliquity and precession for the last 5,000,000 years. ASTRON & ASTROPHYS **51,** 127–35.

Berger, A. 1978. Long term variations of daily insolation and Quaternary Climatic changes. J ATOMS SCI **35,** 2362–7.

Berger, A. 1984. Accuracy and frequency stability of the Earth's orbital elements during the Quaternary. *In* Berger, A., Imbrie, J., Hays, J. D., Kukla, G. & Saltzman, B. (eds) *Milankovitch and Climate,* pp. 3–39. Hingham, Mass.: D. Reidel.

Berger, A. 1988. Milankovitch theory and climate. REVS GEOPHYS **26,** 624–57.

Berger, A. 1989. THIRD INTERNATIONAL CONFERENCE ON PALEO-OCEANOGRAPHY, 16.

Berger, A. & Loutre, M. F. 1988. New insolation values for the climate of the last 10 million years. *Scientific Report 1988/13. Institut d'Astronomie et de Geophysique Georges Lemaitre. Universite Catholique de Louvain-la-Neuve.*

Berggren, W. A., Kent, D. V. & Flynn, J. J. 1985. Jurassic to Paleogene: Part 2, Paleogene geochronology and chronostratigraphy. *In* Snelling, N. J. (ed.) *The Chronology of the Geological Record,* GEOL SOC MEM **10,** 141–95.

Broecker, W. S. 1966. Absolute dating and the astronomical theory of glaciation. SCIENCE **151,** 299–304.

Broecker, W. S., Thurber, D. L., Goddard, J., Ku, T. L., Matthews, R. K. & Mesolella, K. J. 1968. Milankovitch hypothesis supported by precise dating of coral reefs and deep-sea sediments. SCIENCE **159,** 297–300.

Emiliani, C. 1958. Paleotemperature analysis of core 280 and Pleistocene correlations. J GEOL **66,** 264–75.

Emiliani, C. 1955. Pleistocene temperatures. J GEOL **63,** 538–78.

Hays, J. D., Imbrie, J. & Shackleton, N. J. 1976. Variations in the earth's orbit: pacemaker of the ice ages. SCIENCE **194,** 1121–31.

Hilgen, F. J. & Langereis, C. G. 1989. Periodicities of $CaCO_3$ cycles in the Pliocene of Sicily: discrepancies with the quasi-periodicities of the Earth's orbital cycles. TERRA NOVA **1,** 409–415.

Imbrie, J. & Imbrie, J. Z. 1980. Modeling the climatic response to orbital variations. SCIENCE **207,** 943–53.

Imbrie, J., Hays, J. D., Martinson, D. G., McIntyre, A., Mix, A., Morley, J. J., Pisias, N. G. Prell, W. & Shackleton, N. J. 1984. The orbital theory of Pleistocene climate: support from a revised chronology of the marine $\delta^{18}O$ record. *In* Berger, A., Imbrie, J., Hays, J. D., Kukla, G. & Saltzman, B. *Milankovitch and Climate,* pp. 269–305. Hingham, Mass.: D. Reidel.

Jenkins, G. M. & Watts, D. G. 1968. *Spectral Analysis and its Applications.* San Francisco: Holden Day.

Johnson, R. G. 1982. Brunhes–Matuyama magnetic reversal dated at 790,000 yr B.P. by marine-astronomical correlations. QUATERN RES **17,** 135–47.

Maniken, E. A. & Grommé, C. S. 1982. Paleomagnetic data from the Coso Range, California and current status of the Cobb Mountain normal Geomagnetic Polarity Event. GEOPHYS RES LETT **9,** 1279–82.

Martinson, D. G., Pisias, N., Hays, J. D., Imbrie, J., Moore, T. C. & Shackleton, N. J. 1987. Age dating and the orbital theory of the ice ages: development of a high-resolution 0 to 300,000-year chronostratigraphy. QUATERN RES **27,** 1–30.

Milankovitch, M. 1930. Mathematische Klimalehre und astronomische Theorie der Klimaschwankungen. In Köppen, W. & Geiger, R. (eds) *Handbuch der Klimatologie*, I (A), pp. 1–176. Berlin: Gebrüder Borntraeger.

Morley, J. J. & Shackleton, N. J. 1984. The effect of accumulation rate on the spectrum of geologic time series: evidence from two South Atlantic sediment cores. *In* Berger, A. L. *et al.* (eds) *Milankovitch and Climate,* Part 1, pp. 467–480. Hingham, Mass.: D. Reidel.

Nelson, C. S., Hendy, C. H., Cuthbertson, A. M. & Jarrett, G. R. 1986. Late Quaternary carbonate and isotope stratigraphy, subantarctic Site 594, southwest Pacific. INITIAL REPORTS OF THE DEEP SEA DRILLING PROJECT **90,** 1425–36.

Ninkovitch, D. & Shackleton, N. J. 1975. Distribution, stratigraphic position and age of ash layer "L", in the Panama Basin region. EARTH AND PLANET SCI LETT **27,** 20–34.

Peng, T.-S., Broecker, W. S., Kipphut, G. & Shackleton, N. J. 1977. The relation of sediment mixing to the distortion of climatic records in the deep sea sediments. *In* Andersen, N. R. & Malahoff, A. (eds) *The Fate of Fossil Fuel CO_2 in the Oceans*. New York: Plenum.

Pisias, N., Martinson, D. G., Moore, T. C. Jr., Shackleton, N. J., Prell, W., Hays, J. D. & Boden, G. 1984. High resolution stratigraphic correlations of benthic oxygen isotopic records spanning the last 300,000 years. MAR GEOL **56,** 119–36.

Prell, W., Imbrie, J., Martinson, D. G., Morley, J., Pisias, N., Shackleton, N. J. & Streeter, H. 1986. Graphic correlation of oxygen isotope stratigraphy application to the late Quaternary. PALEOCEANOGR **1,** 137–62.

Raymo, M. E., Ruddiman, W. F., Backman, J., Clement, B. M. & Martinson, D. G. 1989. Late Pliocene variations in northern hemisphere ice sheets and North Atlantic deep water circulation. PALEOCEANOGR **4,** 413–46.

Raymo, M. E., Ruddiman, W. F., Shackleton, N. J. & Oppo, D. W. 1990. Evolution of global ice volume and Atlantic-Pacific $\delta^{13}C$ gradients over the last 2·5 M.Y. EARTH AND PLANET SCI LETT **97,** 353–68.

Ruddiman, W. F., McIntyre, A. & Raymo, M. E. 1986. Matuyama 41,000-year cycles: North Atlantic Ocean and northern hemisphere ice sheets. EARTH AND PLANET SCI LETT **80,** 117–29.

Ruddiman, W. F., Cameron, D. & Clement, B. M. 1987. Sediment disturbance and correlation of offset holes drilled with the hydraulic piston corer. *In* Ruddiman, W. F., Kidd, R. B., Thomas, E., *et al.* (eds) INITIAL REPORTS OF THE DEEP SEA DRILLING PROJECT, **94,** pp. 615–634. Washington: U.S. Government Printing Office.

Ruddiman, W. F., Raymo, M. E., Martinson, D. G., Clement, B. M. & Backman, J. 1989. Pleistocene evolution: Northern hemisphere ice sheets and North Atlantic Ocean. PALEOCEANOGR **4,** 353–412.

Shackleton, N. J. 1969. The last interglacial in the marine and terrestrial records. PROC R SOC LOND (B) **174,** 135–54.

Shackleton, N. J. 1977. Carbon-13 in Uvigerina: tropical rainforest history and the Equatorial Pacific carbonate dissolution cycles. *In* Andersen, N. R. & Malahoff, A. (eds) *The Fate of Fossil Fuel CO_2 in the Oceans*. pp. 401–27. New York: Plenum.

Shackleton, N. J. & Hall, M. A. 1983. Stable isotope record of Hole 504 sediments: high-resolution record of the Pleistocene. *In* Cann, J. R., Langseth, M. G. *et al.* (eds) INITIAL REPORTS OF THE DEEP SEA DRILLING PROJECT **69,** 431–441.

Shackleton, N. J. & Hall, M. A. 1989. Stable isotope history of the Pleistocene at ODP Site 677. *In* Becker, K., Sakai, H. *et al.* (eds) PROC ODP, SCI RESULTS **111,** College Station, TX, 295–316.

Shackleton, N. J. & Opdyke, N. D. 1973. Oxygen isotope and palaeomagnetic stratigraphy of equatorial Pacific core V28-238: oxygen isotope temperatures and ice volumes on a 105 and 106 year scale. QUATERN RES **3,** 39–55.

Shackleton, N. J. & Opdyke, N. D. 1976. Oxygen isotope and paleomagnetic stratigraphy of Pacific core V28-239, Late Pliocene to Latest Pleistocene. *In* Cline, R. M. & Hays, J. D. (eds) *Investigation of Late Quaternary Paleoceanography and Paleoclimatology,* GEOL SOC AMER MEM **145,** 449–64.

Shackleton, N. J. & Pisias, N. G. 1985. Atmospheric carbon dioxide, orbital forcing and climate. *In* Sundquist, E. T. & Broecker, W. S. (eds) *The Carbon Cycle and Atmospheric CO_2: Natural Variations Archaean to Present.* GEOPHYS MONOGR **32,** 303–317. American Geophysical Union, Washington, D.C.

Shackleton, N. J., Backman, J., Zimmerman, H. B., Kent, D. V., Hall, M. A., Roberts, D. G., Schnitker, D., Baldauf, J. G., Despraires, A., Homrighausen, R., Huddlestun, P., Keene, J. B., Kaltenback, A. J., Krumsiek, K. A. O., Morton, A. C., Murray, J. W. & Westberg-Smith, J. 1984. Oxygen isotope calibration of the onset of ice-rafting and history of glaciation in the North Atlantic region. NATURE **307,** 620–3.

Shipboard Scientific Party, 1988. Sites 677 and 678. *In* Becker, K., Sakai, H. *et al.* (eds) PROC ODP INIT REPTS (Pt A) **111,** 253–346.

Steiger, R. H. & Jäger, E. 1977. Subcommission on Geochronology: convention on the use of decay constants in geo- and cosmochronology. EARTH PLANET SCI LETT **36,** 359–62.

N. J. SHACKLETON, Subdepartment of Quaternary Research, The Godwin Laboratory, Free School Lane, Cambridge CB2 3RS, U.K.
A. BERGER, Institut d'Astronomie et de Géophysique G. Lemaitre, Université Catholique de Louvain, Louvain-la-Neuve, Belgium.
W. R. PELTIER, Department of Physics, University of Tornoto, Ontario M5S 1A7, Canada.

MS received 17 October 1989. Accepted for publication 22 May 1990

APPENDIX 1

Additional isotopic data obtained subsequent to the main body of analyses going to press (Shackleton and Hall, 1989).

Laboratory code	Depth (ODP)	$\delta^{18}O$	$\delta^{13}C$
Globigerinoides ruber 300–350μm			
A 89/2417ODP677B	3.10	-1.12	1.29
A 89/2418ODP677B	3.20	-1.20	1.34
A 89/2419ODP677B	3.30	-1.21	1.39
A 89/2420ODP677B	3.40	-1.43	1.51
A 89/2421ODP677B	3.50	-1.59	1.52
A 89/2422ODP677B	3.60	-1.66	1.68
A 89/2423ODP677B	3.70	-1.83	1.64
A 89/2424ODP677B	3.80	-1.91	1.65
A 89/2425ODP677B	3.90	-1.79	1.59
A 89/2426ODP677B	3.98	-1.58	1.47
A 89/2427ODP677B	4.10	-1.18	1.74
A 89/2428ODP677B	4.20	-1.66	1.67
A 89/2429ODP677B	4.30	-1.74	1.85
A 89/2430ODP677B	4.40	-1.71	1.74
A 89/2431ODP677B	4.60	-1.91	1.68
A 89/2432ODP677B	4.70	-1.85	1.55
A 89/2433ODP677B	4.80	-1.73	1.47
A 89/2434ODP677B	4.90	-1.44	1.71
A 89/2435ODP677B	5.00	-1.81	1.38
A 89/2436ODP677B	5.10	-1.83	1.52
A 89/2437ODP677B	5.20	-1.73	1.68
A 89/2438ODP677B	5.30	-2.50	1.35
A 89/2439ODP677B	5.40	-1.70	1.18
A 89/2281ODP677B	26.10	-0.94	1.10
A 89/2282ODP677B	26.20	-1.17	1.35
A 89/2283ODP677B	26.30	-1.29	1.36
A 89/2284ODP677B	26.40	-1.45	1.23
A 89/2285ODP677B	31.15	-0.83	0.92
A 89/2286ODP677B	31.25	-0.75	0.85
A 89/2287ODP677B	31.35	-0.69	0.87
A 89/2288ODP677B	31.48	-0.68	1.04
A 89/2289ODP677B	31.55	-0.73	1.04
A 89/2290ODP677B	31.65	-0.75	0.97
A 89/2291ODP677B	31.75	-0.92	1.03
A 89/2292ODP677B	31.81	-1.30	1.00
A 89/2293ODP677B	31.95	-1.30	1.01
A 89/2294ODP677B	32.05	-1.34	0.93
A 89/2295ODP677B	32.18	-1.25	0.80
A 89/2296ODP677B	32.25	-1.36	0.61
A 89/2297ODP677B	32.33	-0.80	0.60

Laboratory code	Depth (ODP)	$\delta^{18}O$	$\delta^{13}C$
Globigerinoides ruber 300–350μm (*contd*)			
A 89/2298ODP677B	32.45	-0.96	0.73
A 89/2299ODP677B	32.55	-0.95	0.88
A 89/2300ODP677B	32.65	-1.03	1.04
A 89/2301ODP677B	32.75	-1.16	0.99
A 89/2303ODP677B	32.95	-1.25	1.07
A 89/2448ODP677B	32.95	-1.26	1.46
A 89/2304ODP677B	33.05	-1.43	1.02
A 89/2449ODP677B	33.15	-1.34	1.51
A 89/2306ODP677B	33.25	-1.36	1.27
A 89/2307ODP677B	33.37	-1.72	1.60
A 89/2308ODP677B	33.45	-1.35	1.46
A 89/2309ODP677B	33.55	-1.55	1.61
A 89/2310ODP677B	33.68	-1.76	1.63
A 89/2440ODP677B	33.75	-1.89	1.64
A 89/2441ODP677B	33.86	-1.73	1.35
A 89/2442ODP677B	33.95	-2.24	1.13
A 89/2443ODP677B	34.05	-1.61	1.15
A 89/2376ODP677B	40.65	-1.14	1.16
A 89/2377ODP677B	40.75	-0.97	0.91
A 89/2378ODP677B	40.83	-0.96	0.75
A 89/2450ODP677B	40.98	-0.98	1.00
A 89/2380ODP677B	41.05	-1.19	0.91
A 89/2381ODP677B	41.15	-1.18	0.76
A 89/2382ODP677B	41.25	-1.10	1.10
A 89/2383ODP677B	41.36	-1.43	1.15
A 89/2384ODP677B	41.47	-1.34	1.03
A 89/2385ODP677B	41.55	-1.17	1.37
A 89/2386ODP677B	41.68	-1.40	1.34
A 89/2387ODP677B	41.75	-1.37	1.39
A 89/2388ODP677B	41.86	-1.71	1.46
A 89/2389ODP677B	41.96	-1.55	1.42
A 89/2390ODP677B	42.05	-1.48	1.55
A 89/2361ODP677B	42.15	-1.64	1.69
A 89/2362ODP677B	42.25	-1.56	1.84
A 89/2363ODP677B	42.36	-1.64	1.79
A 89/2365ODP677B	42.45	-1.67	1.68
A 89/2364ODP677B	42.55	-1.91	1.78
A 89/2366ODP677B	42.65	-1.83	1.85
A 89/2367ODP677B	42.75	-1.99	1.89
A 89/2368ODP677B	42.86	-1.87	1.68
A 89/2369ODP677B	42.96	-1.80	1.81
A 89/2370ODP677B	43.05	-1.66	1.83
A 89/2372ODP677B	43.18	-1.83	1.60
A 89/2445ODP677B	43.25	-1.43	1.47
A 89/2373ODP677B	43.36	-1.38	1.69
A 89/2374ODP677B	43.45	-1.51	1.48
A 89/2375ODP677B	43.55	-1.44	1.52
A 89/2391ODP677B	50.15	-1.68	1.17
A 89/2392ODP677B	50.25	-1.36	1.01
A 89/2393ODP677B	50.35	-1.26	0.93
A 89/2394ODP677B	50.48	-1.23	0.79
A 89/2395ODP677B	50.55	-1.26	1.06
A 89/2396ODP677B	50.65	-1.41	1.15
A 89/2398ODP677B	50.85	-1.38	1.27
A 89/2399ODP677B	50.95	-1.52	1.33
A 89/2400ODP677B	51.05	-1.53	1.26
A 89/2401ODP677B	51.15	-1.41	0.96
A 89/2402ODP677B	51.65	-1.44	1.25
A 89/2403ODP677B	51.75	-1.34	1.14
A 89/2404ODP677B	51.85	-1.84	1.38
A 89/2405ODP677B	51.95	-1.93	1.38
A 89/2406ODP677B	52.05	-1.75	1.60
A 89/2407ODP677B	52.15	-1.73	1.42
A 89/2408ODP677B	52.25	-1.59	1.67
A 89/2409ODP677B	52.35	-1.91	1.48
A 89/2410ODP677B	52.45	-1.61	1.58
A 89/2411ODP677B	52.55	-1.61	1.58
A 89/2412ODP677B	52.67	-1.82	1.39
A 89/2413ODP677B	52.75	-1.85	1.37
A 89/2446ODP677B	52.85	-1.87	1.22
A 89/2415ODP677B	52.95	-1.83	1.44
A 89/2447ODP677B	53.05	-1.74	1.30
A 89/2444ODP677B	64.10	-1.13	0.86
Uvigerina senticosa			
A 89/2340ODP677B	4.40	3.83	-0.98
A 89/2331ODP677B	4.60	3.85	-1.07
A 89/2332ODP677B	4.70	3.99	-1.14
A 89/2333ODP677B	4.80	4.14	-1.13
A 89/2334ODP677B	4.90	3.48	-1.17
A 89/2335ODP677B	5.00	3.72	-1.12
A 89/2337ODP677B	5.20	3.95	-1.01
A 89/2338ODP677B	5.30	3.65	-1.07
A 89/2339ODP677B	5.40	3.83	-0.98
A 89/2161ODP677B	26.10	4.37	-1.28
A 89/2261ODP677B	26.20	4.18	-1.31
A 89/2163ODP677B	26.30	4.16	-1.27
A 89/2164ODP677B	26.40	4.00	-0.87
A 89/2262ODP677B	31.15	4.36	-1.54
A 89/2165ODP677B	31.15	3.30*	-1.75
A 89/2166ODP677B	31.25	4.40	-1.64
A 89/2167ODP677B	31.35	4.35	-1.64
A 89/2168ODP677B	31.48	4.36	-1.44
A 89/2170ODP677B	31.55	4.42	-1.60
A 89/2171ODP677B	31.65	4.29	-1.46
A 89/2172ODP677B	31.75	4.28	-1.66
A 89/2173ODP677B	31.81	4.01	-1.49
A 89/2174ODP677B	31.95	4.13	-1.39
A 89/2175ODP677B	32.05	3.98	-1.59
A 89/2176ODP677B	32.18	4.09	-1.69
A 89/2177ODP677B	32.25	4.10	-1.74
A 89/2178ODP677B	32.33	4.16	-1.73
A 89/2179ODP677B	32.45	4.40	-1.75
A 89/2180ODP677B	32.55	4.41	-1.74
A 89/2181ODP677B	32.65	4.29	-1.36
A 89/2182ODP677B	32.75	4.29	-1.60
A 89/2183ODP677B	32.86	4.02	-1.76
A 89/2184ODP677B	32.95	4.05	-1.70
A 89/2185ODP677B	33.05	3.96	-1.60
A 89/2186ODP677B	33.15	3.83	-1.45
A 89/2187ODP677B	33.25	3.63	-1.54
A 89/2188ODP677B	33.37	3.71	-1.81
A 89/2189ODP677B	33.45	3.61	-1.34
A 89/2190ODP677B	33.55	3.53	-1.15
A 89/2195ODP677B	33.86	3.26	-1.48

Laboratory code	Depth (ODP)	$\delta^{18}O$	$\delta^{13}C$
Uvigerina senticosa (*contd*)			
A 89/2196ODP677B	33.95	3.40	-1.42
A 89/2197ODP677B	34.05	3.34	-1.52
A 89/2327ODP677B	34.10	3.61	-1.77
A 89/2328ODP677B	34.20	4.11	-1.66
A 89/2329ODP677B	34.30	4.20	-1.73
A 89/2214ODP677B	40.65	4.18	-1.54
A 89/2215ODP677B	40.75	4.17	-1.61
A 89/2216ODP677B	40.83	4.40	-1.51
A 89/2217ODP677B	40.98	4.35	-1.60
A 89/2218ODP677B	41.05	4.38	-1.57
A 89/2220ODP677B	41.25	4.33	-1.47
A 89/2223ODP677B	41.55	3.85	-1.37
A 89/2224ODP677B	41.68	3.91	-1.36
A 89/2225ODP677B	41.75	3.95	-1.46
A 89/2226ODP677B	41.86	3.80	-1.22
A 89/2227ODP677B	41.96	3.80	-1.24
A 89/2228ODP677B	42.05	3.78	-1.29
A 89/2198ODP677B	42.15	3.73	-1.30
A 89/2199ODP677B	42.25	3.78	-1.16
A 89/2200ODP677B	42.36	3.76	-1.00
A 89/2201ODP677B	42.45	3.77	-1.11
A 89/2202ODP677B	42.55	3.53	-1.23
A 89/2203ODP677B	42.65	3.54	-1.17
A 89/2204ODP677B	42.75	3.58	-1.08
A 89/2205ODP677B	42.86	3.62	-1.00
A 89/2206ODP677B	42.96	3.38	-1.03
A 89/2208ODP677B	43.05	3.51	-1.02
A 89/2209ODP677B	43.18	3.63	-0.91
A 89/2210ODP677B	43.25	3.68	-1.19
A 89/2211ODP677B	43.36	3.65	-1.03
A 89/2212ODP677B	43.45	3.68	-1.12
A 89/2213ODP677B	43.55	3.68	-1.00
A 89/2311ODP677B	43.60	3.20	-0.55
A 89/2316ODP677B	44.10	4.07	-1.44
A 89/2318ODP677B	44.30	4.31	-1.65
A 89/2321ODP677B	44.50	4.21	-1.70
A 89/2322ODP677B	44.60	4.26	-1.56
A 89/2323ODP677B	44.70	4.29	-1.62
A 89/2324ODP677B	44.80	4.16	-1.62
A 89/2325ODP677B	44.90	4.12	-1.56
A 89/2326ODP677B	45.00	4.00	-1.63
A 89/2240ODP677B	49.55	3.81	-1.56
A 89/2241ODP677B	49.68	3.90	-1.53
A 89/2242ODP677B	49.75	3.36	-1.14
A 89/2245ODP677B	50.05	3.23	-1.39
A 89/2246ODP677B	50.15	3.34	-1.47
A 89/2247ODP677B	50.25	3.58	-1.57
A 89/2248ODP677B	50.35	3.71	-1.57
A 89/2249ODP677B	50.48	3.84	-1.53
A 89/2250ODP677B	50.55	3.96	-1.75
A 89/2251ODP677B	50.65	3.95	-1.66
A 89/2252ODP677B	50.75	3.86	-1.57
A 89/2253ODP677B	50.85	4.10	-1.66
A 89/2254ODP677B	50.95	4.10	-1.52
A 89/2255ODP677B	51.05	3.81	-1.31
A 89/2256ODP677B	51.15	4.02	-1.45
A 89/2258ODP677B	51.65	3.90	-1.43
A 89/2259ODP677B	51.75	4.00	-1.65
A 89/2260ODP677B	51.85	3.63	-1.09
A 89/2270ODP677B	52.25	3.53	-1.06
A 89/2231ODP677B	64.20	4.28	-1.53
A 89/2233ODP677B	64.40	4.15	-1.27
A 89/2234ODP677B	64.50	4.04	-1.40
A 89/2235ODP677B	64.60	3.94	-1.38
A 89/2236ODP677B	64.70	3.86	-1.34
A 89/2237ODP677B	64.80	3.69	-1.25
A 89/2238ODP677B	64.90	3.86	-1.35
Cibicidoides wuellerstorfi			
A 89/2257ODP677B	51.15	3.47	-0.49
A 89/2280ODP677B	52.95	3.00	-0.24
A 89/2271ODP677B	53.05	2.91	-0.32
A 89/2229ODP677B	64.10	3.53	-0.76
A 89/2232ODP677B	64.30	3.58	-0.74
A 89/2239ODP677B	64.90	3.02	-0.49
Cibicidoides spp.			
A 89/2192ODP677B	33.68	2.91	-0.61
A 89/2193ODP677B	33.75	2.57	-0.23
A 89/2314ODP677B	43.90	3.20	-0.46
Oridorsalis spp.			
A 89/2336ODP677B	5.10	3.88	-1.48
A 89/2169ODP677B	31.48	4.34	-1.91
A 89/2263ODP677B	31.15	4.44	-2.05
A 89/2244ODP677B	49.95	3.21	-1.58
A 89/2265ODP677B	51.95	3.51	-1.50
A 89/2275ODP677B	52.55	3.32	-1.54
Hoeglundina elegans			
A 89/2264ODP677B	31.15	5.18	0.50
Globobulimina pacifica			
A 89/2191ODP677B	33.68	3.54	-2.44
A 89/2243ODP677B	49.83	3.47	-2.43
A 89/2268ODP677B	52.15	3.82	-2.21
Globocassidulina subglobosa			
A 89/2266ODP677B	52.05	3.59	-0.90
A 89/2276ODP677B	52.67	3.38	-1.12
Sphaeroidina bulloides			
A 89/2269ODP677B	52.15	3.44	-0.67
A 89/2273ODP677B	52.45	3.42	-0.78
A 89/2274ODP677B	52.55	3.45	-0.84
A 89/2277ODP677B	52.67	3.41	-0.70
A 89/2278ODP677B	52.75	3.56	-0.70
mixtures of Oridorsalis, Globobulimina, Sphaeroidina, Uvigerina, Globocassidulina			
A 89/2194ODP677B	33.75	3.24	-1.64
A 89/2330ODP677B	34.40	4.44	-1.45
A 89/2219ODP677B	41.15	3.60	-2.61
A 89/2315ODP677B	44.00	3.73	-1.75
A 89/2317ODP677B	44.20	4.13	-2.01
A 89/2267ODP677B	52.05	3.79	-1.84
A 89/2272ODP677B	52.35	3.57	-1.81
A 89/2279ODP677B	52.85	3.52	-0.99